ELSEVIER

Catena 25 (1995) 227–252

CATENA

Hydrological structure and erosion damage caused by concentrated flow in cultivated catchments

Bruno Ludwig [a], Jean Boiffin [a], Joël Chadœuf [b], Anne-Véronique Auzet [c]

[a] *INRA — Unité d'Agronomie de Laon, rue Fernand Christ, F-02007 Laon Cedex, France*
[b] *INRA — Laboratoire de Biométrie, Site Agroparc, F-84914 Avignon Cedex 9, France*
[c] *CEREG-URA 95 CNRS, Université Louis Pasteur, 3 rue de l'Argonne, F-67083 Strasbourg Cedex, France*

Received 15 November 1993; accepted after revision 10 September 1994

Abstract

This study analyses the between-catchment variability of rill volumes produced by concentrated flow erosion during winter in the northern part of the Paris Basin. The working hypotheses were that (i) runoff concentrates along channels determined by topography or by agricultural practices; (ii) rill length is a major component of rill volume variability on a catchment scale; (iii) rill cross-sectional areas are controlled by the size of upslope runoff-contributing areas connected to the corresponding channels. Two samples, one of 20 zero order catchments and the other of 15 catchments, were surveyed. For each catchment, the runoff collector network was modelled from topographical and agricultural information, and split into homogeneous segments. Each segment was characterized by its slope gradient (**SL**), the soil susceptibility to rill erosion (**SSE**) and the size of the upslope runoff-contributing areas (**RCA**) connected to it. These areas were identified by the structural state of their soil surface. The frequency of rill occurrence was highly correlated with **RCA** and **SL**. The rill cross-sectional areas of eroded channels were correlated with **RCA**, **SL** and **SSE**. Catchment erosion rates were estimated by adding together the predicted rill volumes for each segment within the catchment. These estimations were closely correlated with observed rill erosion rates. The relative spatial position of runoff-contributing areas and runoff collectors must be taken into account when examining the damage caused by concentrated flow erosion.

1. Introduction

Concentrated flow erosion is a subject of increasing interest to soil conservationists in North Western Europe because of its frequency, the severity of associated off-site damage, and the relative lack of information on this type of erosion. Concentrated flow

SSDI 0341-8162(95)00012-7

erosion is particularly widespread on loamy plateaus occupied by intensive agriculture, such as the Pays de Caux in France (Papy and Douyer, 1991), the South Downs in England (Boardman, 1990), and Central Belgium (Poesen and Govers, 1990). In such areas, deep, large ephemeral gullies may appear even where slope gradients and rainfall intensities are relatively low. Cropping systems are believed to be at least partly responsible for this severe environmental problem, but the links between agricultural management and erosion are complex and sometimes ambivalent (Monnier et al., 1986; Auzet et al., 1990; Imeson and Kwaad, 1990; Ouvry, 1990). This is especially true for concentrated flow erosion because the areas generating runoff can differ spatially from those supplying sediments (Boiffin et al., 1988a; Auzet et al., 1990). The processes involved in runoff generation, flow concentration and soil detachment by running water must be carefully analysed to understand the interactive effects of physical and agricultural characteristics in order to design adequate protective measures.

Concentrated flow erosion results from the hydrological connection between a runoff-contributing area where soil detachment does not necessarily occur and a collecting channel where flow discharge and velocity exceed the critical values for rill initiation and development (Govers, 1985; Rauws and Govers, 1988; Foster, 1990; Moore and Foster, 1990). The properties determining the capacity of the land to produce runoff (i.e. soil infiltrability and surface storage) are strongly influenced by the structure of topsoil layers (Monnier and Boiffin, 1986; Monnier et al., 1986). Interactions between farm operations, climate and soil texture induce complex, rapid and deep changes in topsoil structure and its hydraulic properties (Boiffin et al., 1988b; Papy and Boiffin, 1989; Imeson and Kwaad, 1990). As a result, the timing of gully initiation is closely correlated with the dynamics of surface structure degradation on upslope surrounding fields by rainfall crusting or by surface wheel compaction (Boiffin et al., 1988a).

These studies led to the selection of criteria for characterizing the soil surface state and identifying fields that are prone to generate runoff, even with low rainfall intensity. Auzet et al. (1995) used these criteria to monitor a sample of catchments for three consecutive winters to estimate the proportion of the catchment area which was presumed to contribute to runoff for most rainfall events. They found that this proportion accounted for a large part (74%) of the variation in erosion rates, both between sites and between years. However, this empirical relationship established at the catchment scale was not accurate enough for a good assessment of rill erosion risks at a given site, since the unexplained part of rill erosion rate variability remained large. Analysis of the residual deviations led to the hypothesis that the spatial position of the contributing areas within the catchment could account for a part of the erosion rate variability. Distant contributing areas can generate very long rills in the talweg, while contributing areas located close to the catchment outlet generate only short rills.

The present study analyses rill volume variability at the catchment scale by considering rill lengths and rill cross-sectional areas as distinct components of rill volumes, each of these components being influenced by specific factors. Rill lengths are determined by the route of the runoff within the catchment, and by the location of the rill heads along this route. The route of the concentrated runoff is determined by both topography and agricultural land-use, which produce different types of linear depression features. Those topographical and agricultural features form a runoff collector network, which guides the

flow towards the catchment outlet and determines the maximum cumulated length of rills produced by concentrated flow. The location of rill heads is determined by the spatial distribution of flow discharge and flow velocities along the runoff collector network during a rainfall event (Moore and Foster, 1990). This spatial distribution depends mainly on the location and size of areas producing runoff and on the way they are connected to the runoff collector network. Rill cross-sectional areas are controlled by flow discharges and velocities along the different collecting channels, which again depend on the relative positions of channels and runoff-contributing areas (Moore and Foster, 1990; Thorne and Zevenbergen, 1990).

It therefore seems very important to take into account the hydrological structure of the catchment in order to understand the variability of erosion by concentrated flow. This was done in four steps.

(i) The hydrological structure of the catchment was determined by identifying the runoff collectors, the runoff-contributing areas and the hydrological connections between these two components. This was done independently from rill observation and characterization. The catchment was then divided into hydrological sub-units associated with specific segments of the runoff collector network.

(ii) Erosion characteristics, i.e. rill presence along a given collector and rill cross-sectional areas were correlated with the characteristics of a given hydrological sub-unit.

(iii) The resulting empirical relationships were used to predict rill volume and erosion rates corresponding to concentrated flow erosion in a catchment.

(iv) The quality of this prediction was compared to that obtained by a correlation of overall erosion rates and average catchment characteristics.

This approach was used to analyse two samples of small catchments having a wide range of topographical, pedological and agricultural characteristics.

2. Material and methods

2.1. Spatial and temporal context

The survey was conducted on zero order catchments. These units were defined by Auzet et al. (1993) as areas hydrologically related to a single main concentration line or talweg, corresponding to an extreme upper branch of a dry valley network. Two samples of catchments were selected in the Northern Paris Basin, within a triangle whose points were Laon (49° 35′N, 3° 35′E), Etretat (49° 40′N, 0° 15′E) and St Omer (50° 45′N, 2° 15′E). The first sample contained 20 catchments and was monitored during the 1989/1990 and 1990/1991 winter seasons, from the beginning of sowing for winter crops to the beginning of seed bed preparation for spring crops. A second sample of 15 catchments was surveyed during the winter of 1991/1992 for testing the conclusions drawn from the first sample. Table 1 shows the main morphological and pedological catchment characteristics. Table 2 gives the land-use patterns, showing that winter crops and tilled intercrops, either ploughed or stubble-ploughed, predominated.

The amount and intensity of rainfall were measured with automatic rain gauges located in such a way that each catchment was no more than 1 km from a rain gauge.

Table 1
Land physical characteristics within the two catchment samples ($n = 35$)

Physical characteristics	mean	min	max
total catchment area (ha)	32.3	3.4	94.7
% of the catchment area with a slope gradient > 5%	35.4	0.3	71.6
% of the catchment area with a slope gradient > 10%	9.5	0.0	50.7
mean slope gradient along the talweg (%)	3.5	1.5	8.5
talweg length (m)	496	50	1890
density of morphological concentration lines (m/ha)	55.4	22.9	112.3
% of the catchment area with a soil prone to crusting [a]	53.2	8.5	100.0
% of the catchment area with a clayey soil surface [b]	3.5	0.0	38.6

[a] A topsoil with a clay content < 17.5%.
[b] A topsoil with a clay content > 30%.

The measurements for the extreme West and extreme East catchments are summarized in Table 3. The between-year variations in rainfall were smaller than the variation between the western and the eastern parts of the study area, especially for rainfalls with intensities above 10 $mm \cdot h^{-1}$. But the time distributions of rainy events were very similar between regions and very different from year to year. Rainfall was concentrated towards the end of the winter in 1989/1990 while it occurred mostly in autumn and in early winter in 1990/1991 and 1991/1992.

2.2. Observations and measurements

2.2.1. Topographical data

A slope map was produced from the contour lines of the 1/25 000 topographic map for each catchment and checked by field measurements using an Abney level, with particular attention to changes in slope gradient, especially for locating the catchment divide.

Each topographical depression line was visually identified and located in relation to field boundaries or particular marks such as roads, hedges or ditches. Perpendicular transects of slope measurements were combined with aerial photographs to map the

Table 2
Land-use characteristics (% of catchment area) within the two catchment samples

	Winter season								
	1989/1990 [a]			1990/1991 [a]			1991/1992 [b]		
Land-use	mean	min	max	mean	min	max	mean	min	max
winter crops	51.8	0.0	100.0	49.0	0.0	99.3	52.9	0.0	100.0
tilled intercrops	36.5	0.0	99.3	39.9	0.0	96.8	300.0	0.0	90.7
non-tilled intercrops	1.6	0.0	17.4	1.4	0.0	11.4	12.1	0.0	100.0
pastures or woods	10.1	0.0	39.5	12.5	0.0	39.5	5.0	0.0	34.2

[a] First sample ($n = 20$).
[b] Second sample ($n = 15$).

Table 3
Rainfall conditions for the three winters studied: **total rainfall** (mm) and *total rainfall at intensities > 10 mm · h⁻¹* (mm)

	Site and winter season					
	Extreme West			Extreme East		
Period	1989/1990	1990/1991	1991/1992	1989/1990	1990/1991	1991/1992
1 Oct.–15 Nov.	**134.3**	**170.6**	**158.7**	**67.0**	**81.7**	**58.7**
	31.9	*58.6*	*29.8*	*10.2*	*9.3*	*7.5*
16 Nov.–15 Jan.	**64.1**	**274.5**	**115.1**	**54.1**	**117.2**	**60.9**
	4.3	*23.7*	*61.0*	*4.7*	*7.8*	*2.1*
16 Jan.–28 Feb.	**210.4**	**37.2**	**44.6**	**96.3**	**10.3**	**15.2**
	23.7	*0.2*	*0.6*	*17.0*	*0.6*	*0.2*
1st Oct.–28 Feb.	**408.8**	**482.3**	**318.4**	**217.4**	**209.2**	**134.8**
	59.9	*82.5*	*91.4*	*31.9*	*17.7*	*9.8*

major depression lines, and particularly the talweg. The precision with which these linear depressions were located varied from about 5 m for the smallest depression lines with a "V" profile to about 50 m for the talwegs with a large concave profile. Fig. 1 shows an example of the map for a catchment from all topographical data.

2.2.2. Soil data

Topsoil textures were determined by manual testing of 4–5 samples per ha, and more frequent sampling around the soil class boundaries. The results of tactile tests were checked by granulometric analyses at a mean rate of 1 analysis for 20 manual tests. Topsoil texture was mapped at a scale of 1/5000 (see Fig. 2). The texture classes refer to the classification commonly used in France (Jamagne, 1967; Baize, 1993).

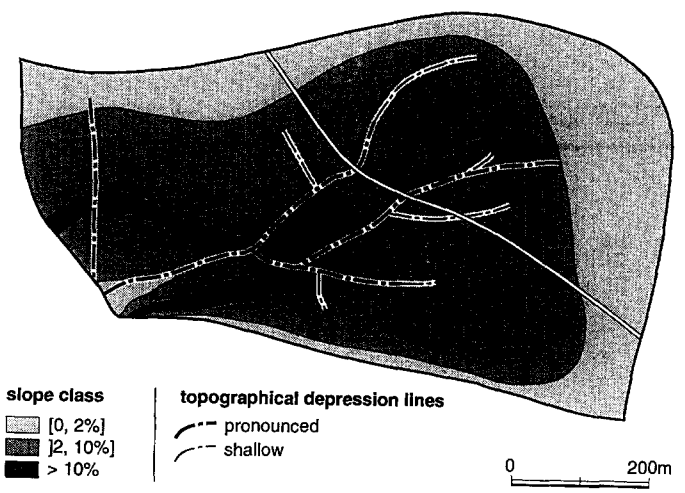

Fig. 1. Topographical characteristics (slope gradient and topographical depression lines).

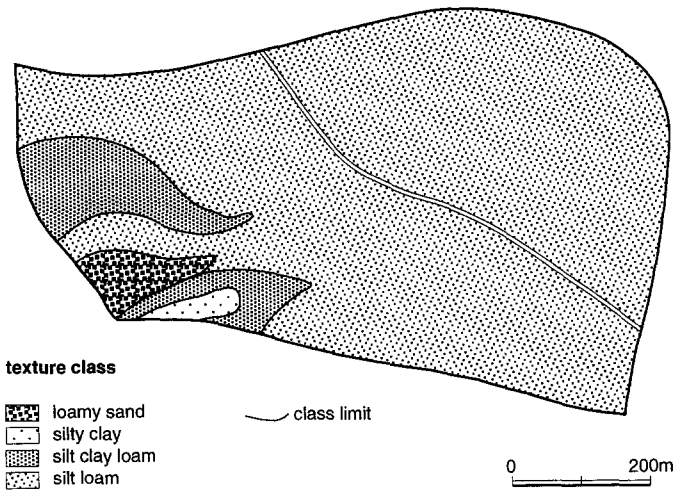

Fig. 2. Texture classes.

2.2.3. Land-use data

Field boundaries, headlands and marked dead furrows (Fig. 3) were mapped. The nature of the crop, the rate of soil cover by growing vegetation and crop residues, the date, nature and direction of the farm operations were noted four to five times during each winter season on each field in each catchment. Fig. 4 shows a map with land-use data for a given catchment.

2.2.4. Soil surface state

Soil surface structure was monitored once a month between October and late February during each winter season. The observations were made on each land unit corresponding to a given class of topsoil texture within a given agricultural field. A total

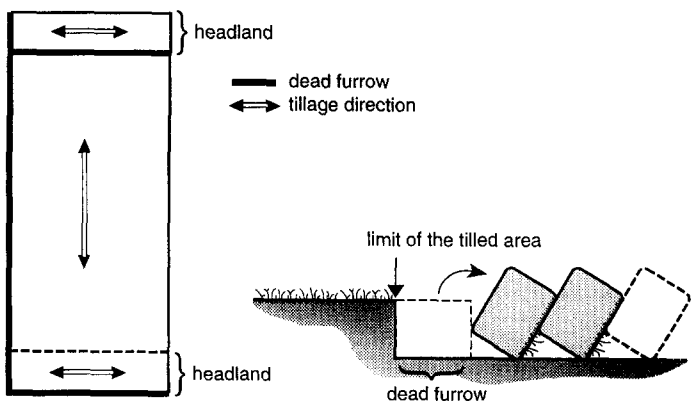

Fig. 3. Location of linear features on a rectangular field.

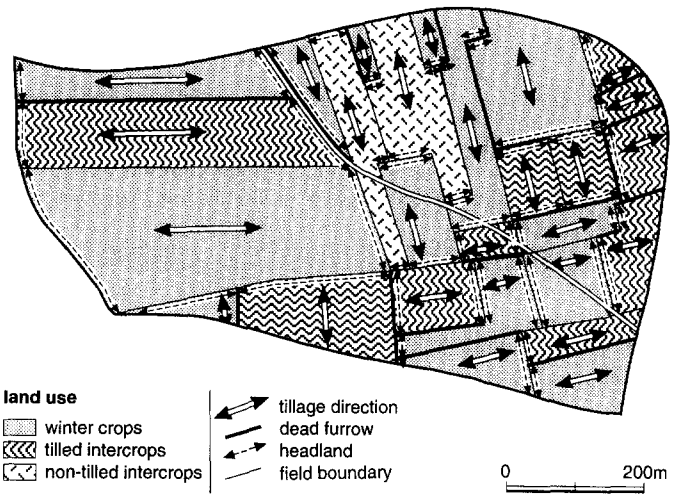

Fig. 4. Land-use and linear agricultural features.

of 600 land units were monitored in 1989/1990, 570 in 1990/1991 and 240 in 1991/1992. The following characteristics were visually assessed: (i) stage of crust development (Table 4), (ii) proportion of land surface covered by wheel tracks, (iii) grading of surface roughness in the tillage direction (Table 5) (Boiffin, 1986; Boiffin et al., 1988a,b).

These data were combined to evaluate the capacity of each land unit in the catchment to produce runoff: a land unit was assumed to be very prone to produce runoff if its roughness grade was R0, with a crusting stage F2 + or if the area covered by wheel tracks was above 50%. Land units having these attributes were denoted as "Runoff-Contributing Areas".

2.2.5. *Rill data*

Each rill was mapped and the rill volume was evaluated from the cross-sectional area, measured every 5–20 m along the rill, and at specific points where the area changed

Table 4
Typical stages of crust development with respect to the extent of structural [a] and depositional [a] crust

Facies	Proportion of soil surface covered by	
	structural crust (%)	depositional crust (%)
F0	0	0
F1	100	0
F1/2	> 50	< 50
F2 −	25–50	50–75
F2	10–25	75–90
F2 +	0–10	90–100

[a] As defined by Chen et al. (1980).

Table 5
Grading of soil surface roughness

Grade	Roughness index [a]	Typical agricultural situation
R0	0–1 cm	strongly crusted sown fields, harvested fields with intense compaction
R1	1–2 cm	sown fields with fine loosened or moderately crusted seedbeds
R2	2–5 cm	recently sown fields with a cloddy surface, crusted tilled fields without residues
R3	5–10 cm	stubble-ploughed fields recently sown fields with a very cloddy surface
R4	> 10 cm	ploughed fields

[a] Difference in the heights of the deepest part of the microdepressions and the lowest point of their divide.

significantly. These measurements were made as late as possible before spring tillage, which could erase some rills: between 12/03 and 22/03 in 1990, 05/03 and 24/03 in 1991 and 19/02 and 26/02 in 1992.

The pattern of each rill was also determined to distinguish erosion caused by concentrated flow from that caused by overland flow (Auzet et al., 1990; Foster, 1986; De Ploey, 1989). Three rill patterns were identified.

1. The "ephemeral gully" pattern (Foster, 1986; Poesen and Govers, 1990; Thorne and Zevenbergen, 1990; Poesen, 1993): rills belonging to this pattern are located on predetermined linear depressions. They are not parallel, their spatial distribution is non-uniform and they originate from a few well-defined rill heads that are irregularly and widely spaced (> 20 m). This pattern was by far the predominant one in our sample; it was found in talweg or in secondary linear depressions draining hillslopes.

2. The "dendritic" pattern: again this pattern has a non-uniform and predetermined space distribution. The rill course is not a single channel, but a dense branching network that gradually converges downwards, each network originating from a number of closely spaced rill heads.

3. The "parallel" pattern: the rills are rather uniformly distributed, they do not converge and their spacing is relatively close (1–20 m) with a periodic trend. This pattern was only found on hillslope and never in the valley bottom.

In the following, the rill volume for the parallel pattern (9–23% of the total rill volume for a winter season) was considered to represent rill–interrill erosion generated by overland flow and not by concentrated flow. It is therefore not taken into account, and only rill volumes for the "ephemeral gully" and "dendritic" patterns were considered to represent concentrated flow erosion.

2.3. Identification and segmentation of the runoff collector network

2.3.1. Network mapping

Topographical and land-use data were combined to identify the runoff collectors independently of rill observations. The runoff collector network was assumed to be composed of all linear depression features liable to concentrate overland flow and to guide the runoff towards the outlet of the catchment. This included topographical depression lines and downslope field borders, provided they were occupied by a dead furrow or a headland. An exception to this rule was made when the maximum slope was

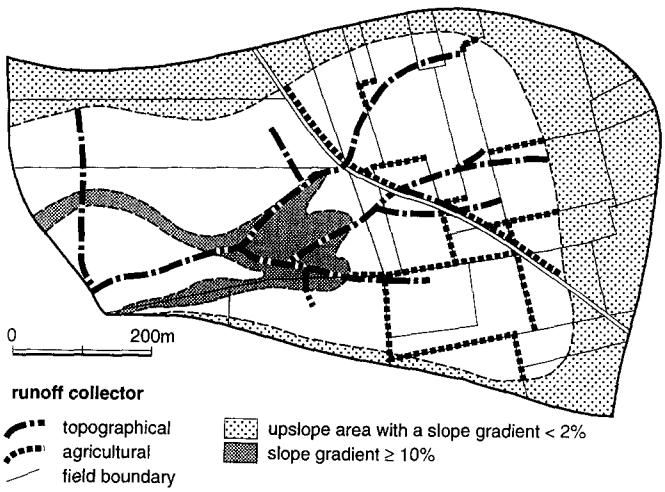

Fig. 5. Runoff collector network formed by topographical and agricultural linear depression features.

above 10% and perpendicular to the headland, and when this headland had no well marked dead furrow. In this particular case, the runoff coming from the field was assumed to pass over the headland without changing its direction.

Runoff collectors were not identified in the upslope part of the catchment with a maximum slope of less than 2%. Erosion was very low in this area (0% to 5% of the total rill volume per catchment), and the topographic information was not accurate enough to predict the runoff directions. The map of the runoff collector network was obtained by combining the topographical and land-use maps (Figs. 1 and 4), as shown in Fig. 5.

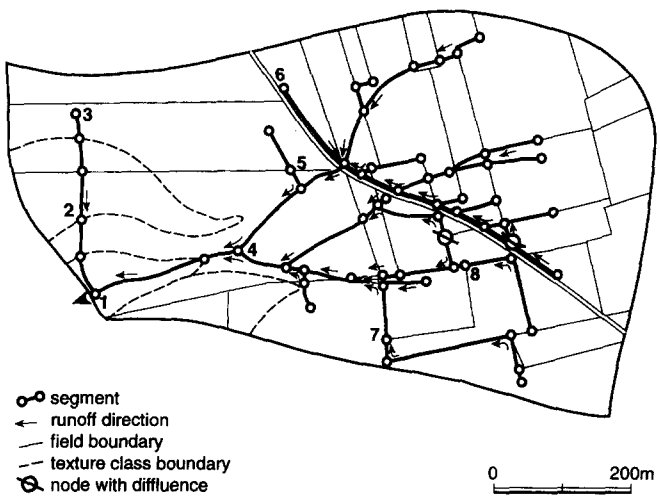

Fig. 6. Segmentation of the runoff collector network.

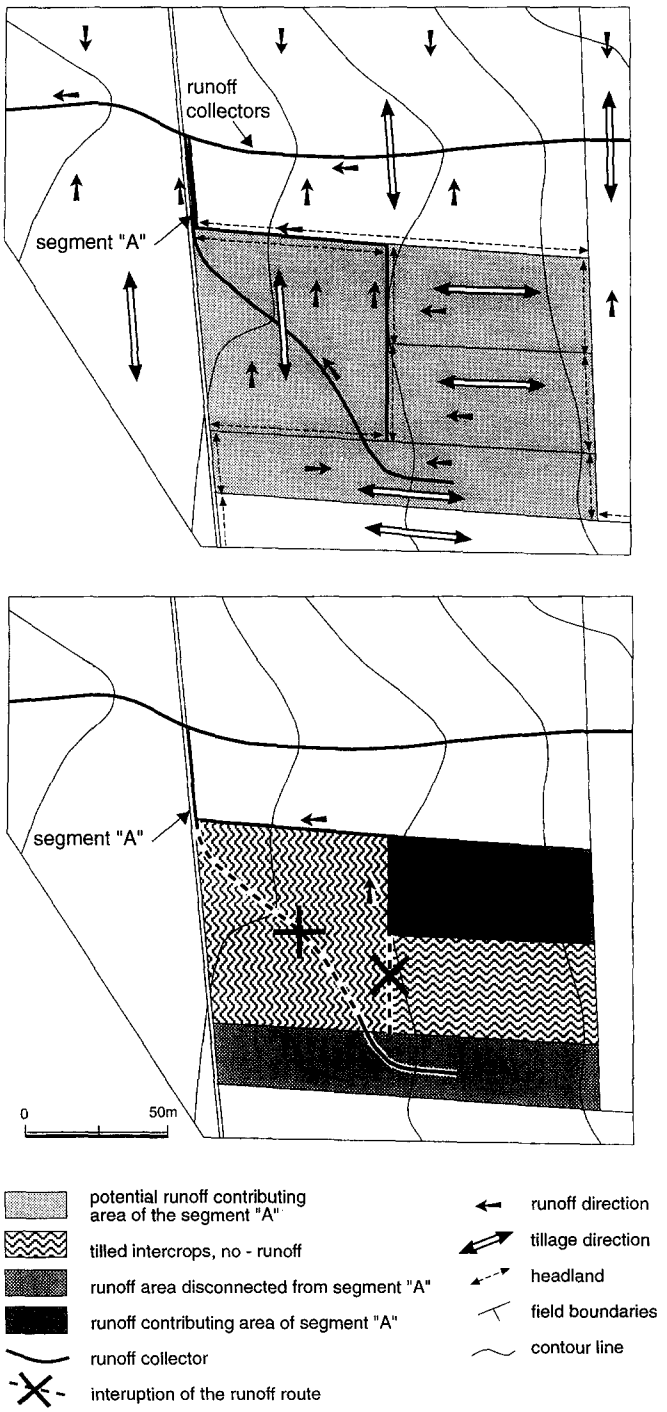

Fig. 7. Identification of the runoff-contributing area connected to a given segment A.

2.3.2. Network segmentation

The runoff collector network was divided into segments (Fig. 6) having uniform runoff and erosion characteristics.

Segment limits were placed as follows:

- at the catchment outlet (e.g. point 1 on Fig. 6);
- at the head of a network branch (e.g. points 3 and 6);
- at a confluence of two network branches (e.g. point 4);
- at an intersection between a collector and a soil textural boundary (e.g. point 2);
- at an intersection between a collector and a field boundary (e.g. points 5, 7 and 8);
- at a sharp change in slope.

Segments delineated in this way were then considered to be the basic spatial units for correlating concentrated flow erosion with the land's physical characteristics.

2.3.3. Segment characterization

The length of each segment was measured on the network map. The runoff-contributing area connected to it, the slope and the soil susceptibility to rill erosion were recorded.

Table 6
Scoring of soil susceptibility to rill erosion (**SSE**) as a function of land-use, topsoil texture and presence of an old filled-in gully. The final grade is given by the three following algorithms:
if $1 \leq G1 + G2 \leq 4$, then $SSE = G1 + G2 + G3$
if $G1 + G2 < 1$, then $SSE = 1 + G3$
if $G1 + G2 > 4$, then $SSE = 4 + G3$

Land-use during autumn, winter and early spring		Grade **G1**
Pasture		+1
Winter crops: cereal or oil seed rape:	% plant cover < 20	+4
	% plant cover 20–40	+3
	% plant cover > 40	+2
Sugar beet or maize (still not harvested)		+2
Spring pea recently sown		+4
Intercrops:		
Previous crop: cereal, oil seed rape:	without tillage after harvest	+1
	stubble-ploughed	+2
	ploughed (fine structure)	+2
	ploughed (blocky structure)	+1
Previous crop: spring pea, flax, maize, sugar beet, carrot:	without tillage after harvest	+1
	surface-tilled	+3
	ploughed (fine structure)	+2
	ploughed (blocky structure)	+1
Topsoil texture		**Grade G2**
< 17.5 % clay and > 17.5 % sand		+1
17.5–30 % clay and > 35 % sand or 7.5–17.5 % clay and < 15 % sand		0
17.5–30 % clay and < 35 % sand		−1
30–45 % clay		−2
Old filled-in gully		**Grade G3**
	no	0
	yes	+1

The runoff-contributing area connected to a given segment was evaluated in several steps. A potential area was first determined from topography and tillage direction (Fig. 7). Only a part of this area was assumed to produce runoff, depending on its soil surface state, as explained in Section 2.2.4. The runoff-contributing areas can be connected to a segment directly or indirectly. Direct connection can occur at the upslope point of the segment or all along it. When the connection occurred at the upslope point of the segment, 100% of the runoff-contributing area was taken into account. When it occurred all along the segment, an "equivalent" runoff-contributing area was approximated to 50% of the actual connected area. An area and a segment can be indirectly connected either via another segment or via a field. High topsoil infiltration capacity and/or high water storage along these intermediary elements could break the hydrological connection. It was then assumed that a permanent pasture, or a recently ploughed or stubble-ploughed field could interrupt the water course, unless a rill was already present before the last important rain event. Some networks had points of runoff diffluence. In such cases, field observations of the runoff direction were made to determine whether only one or both segments actually carried runoff. When both segments were identified as functional, each of them was attributed half the upslope runoff-contributing area.

The slope gradient of 70% of the total number of segments was measured in the field. The slope gradient of the remaining 30% was estimated from the slope map. The average error of these estimates was 0.7% slope gradient, from a sample of 50 measurements made on the map and in the field.

The soil susceptibility to rill erosion depends mainly on the cohesion of topsoil layers, which is determined by the soil bulk density (Lyle and Smerdon, 1965), the soil texture, the soil moisture (Govers et al., 1990; Guerif, 1990) and the density of root armature. A global score was determined (Table 6) for grading this cohesion by combining information on tillage operations, vegetation cover, topsoil texture and the occurrence of old filled-in gullies.

3. Results

3.1. Distribution of segment characteristics

A total of 530 segments were identified in 1989/1990 and 523 in 1990/1991 for the first catchment sample. The second sample contained 301 segments (1991/1992). Each catchment contained 2–55 segments.

The segment characteristics are shown in Fig. 8. The distributions of runoff-contributing areas (**RCA**) were strongly skewed, with a high proportion of zero and very low values, and a tail of high values. The maximum recorded values of **RCA** for the three successive seasons were 20.2, 46.4 and 47.8 ha. The frequency of high **RCA** values was highest in 1990/1991 and lowest in 1989/1990. This between-year difference was correlated with the corresponding rainfall amounts and time distributions. Soil crusts developed much sooner and were thicker in 1990/1991 than in 1989/1990 (Auzet et al., 1995).

The distribution of segment slope gradients (**SL**) was also asymmetric, with more low

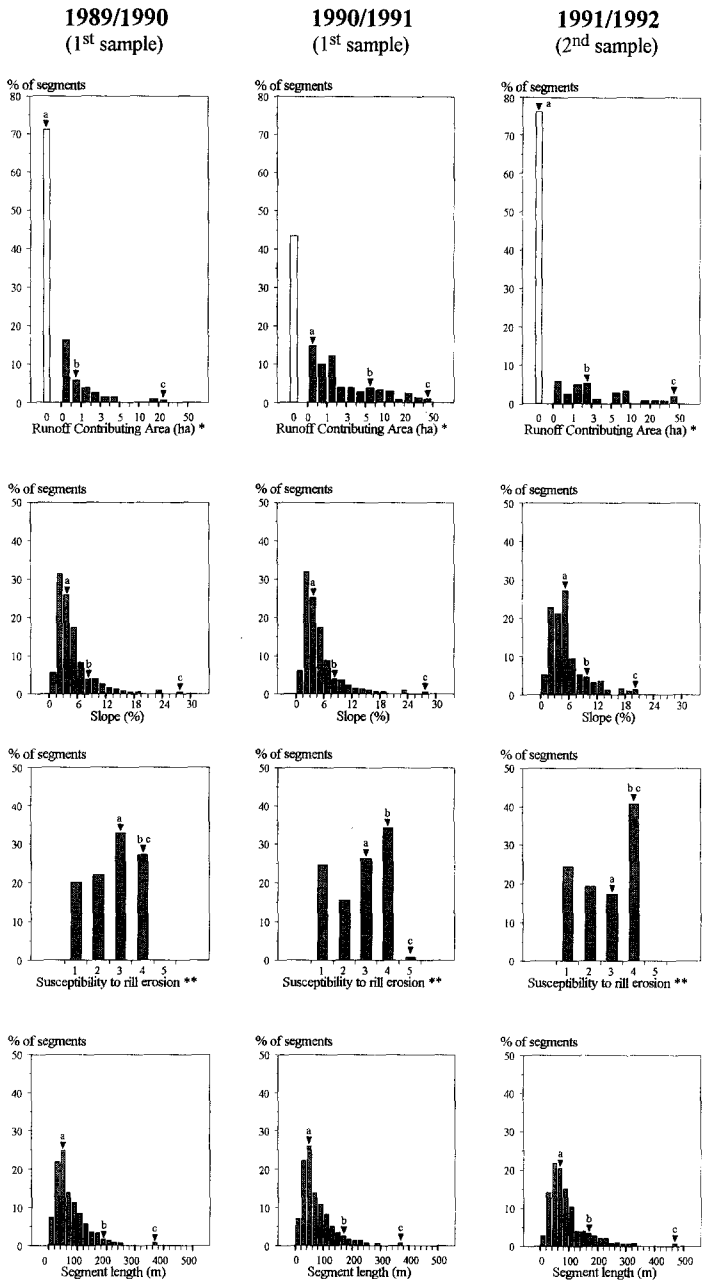

Fig. 8. Distribution of segment characteristics during winters 1989/1990 and 1990/1991 for the first catchment sample and winter 1991/1992 for the second sample.

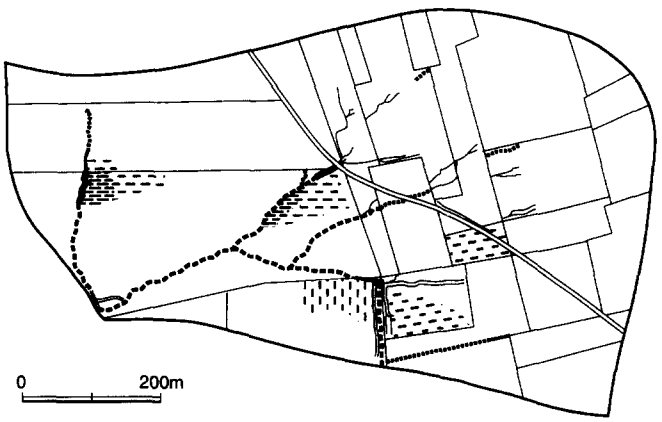

rill pattern	mean cross - sectional area	occurrence of a rill during the study period		
		one winter	two winters	three winters
single channel and dendritic	≥ 500 cm^2			
	< 500 cm^2			
parallel	< 500 cm^2			did not occur

Fig. 9. Location of rills initiated during three winters in a catchment.

values. These low values corresponded either to segments located in the downslope part of the catchments, or to hillslope segments which were almost parallel to the contour lines. The distributions between years and between catchment samples were very similar.

The grades of soil susceptibility to rill erosion (**SSE**) were rather uniformly distributed, except for grade 5 which was very infrequent. There was no marked difference between years. This was consistent with the fact that land-use patterns were very similar from year to year and for the two catchment samples. Land-use was the main factor controlling **SSE**.

The distribution of segment lengths (**L**) was very similar from year to year, with an asymmetric shape and a median value of 60 m for the first catchment sample and 80 m for the second sample. Most segments longer than 150 m were in valley bottoms, which generally had uniform colluvial soil and fields larger than those on hillslopes.

3.2. Relation between rills and runoff collectors

3.2.1. Spatial relations

The rill maps and the maps of runoff collector network showed a clear correlation, e.g. Fig. 9 and Fig. 6. When the rill maps for the first catchment sample in 1989/1990, 1990/1991 and 1988/1989 (data taken from Auzet et al., 1993) were superimposed, the most important rills appeared to be in the same places, or in line with each other

Table 7
Spatial correlation between rill erosion and the runoff collector network

Erosion characterisitics (for a given catchment)		Winter season								
		1989/1990 [a]			1990/1991 [a]			1991/1992 [b]		
		mean	min	max	mean	min	max	mean	min	max
Total rill volume (m^3/ha)	[c]	*0.40*	*0.00*	*2.64*	*2.52*	*0.00*	*11.74*	*0.85*	*0.00*	*8.79*
	[d]	**0.36**	**0.00**	**2.50**	**2.01**	**0.00**	**10.13**	**0.72**	**0.00**	**8.67**
% of rill volume located on the collector network (only for eroded catchment)	[c]	*90.7*	*28.6*	*100.0*	*75.7*	*0.0*	*100.0*	*84.4*	*19.8*	*99.4*
	[d]	**96.7**	**86.2**	**100.0**	**96.6**	**46.9**	**100.0**	**90.5**	**26.4**	**100.0**
Proportion of eroded collectors (% of total network length)	[d]	**10.1**	**0.0**	**37.8**	**25.7**	**0.0**	**83.4**	**18.4**	**0.0**	**77.4**
% of eroded segments	[d]	**14.7**	**0.0**	**66.7**	**27.8**	**0.0**	**81.3**	**18.2**	**0.0**	**74.4**

[a] First catchment sample
[b] Second sample.
[c] *All rill patterns.*
[d] **Only "ephemeral gully" and "dendritic" rill patterns.**

Table 8
Proportion of non-eroded segments according to runoff-contributing area (**RCA**) and segment slope gradient (**SL**)

RCA (ha)	**SL** (%)								
	[0;2[	**[2;3[**	**[3;4[**	**[4;5[**	**[5;6[**	**[6;8[**	**[8;10[**	**[10;15[**	**[15;35[**
0	**0.93**	**0.92**	**0.90**	**0.87**	**0.94**	**0.82**	**0.94**	**0.98**	**1.00**
n	*67*	*103*	*129*	*76*	*77*	*60*	*34*	*40*	*12*
]0;0.5[	**0.75**	**0.81**	**0.81**	**0.70**	**0.68**	**0.88**	**0.64**		
n	*28*	*16*	*21*	*21*	*27*	*16*	*14*		
]0.5;1[	**0.82**	**0.89**	**0.76**	**0.56**	**0.59**		**0.50**		
n	*11*	*18*	*17*	*18*	*17*		*10*		
[1;2[	**0.53**	**0.71**	**0.67**	**0.62**	**0.27**		**0.25**		
n	*19*	*17*	*15*	*13*	*11*		*4*		
[2;7[	**0.40**	**0.20**	**0.29**	**0.22**	**0.10**		**0.10**		
n	*20*	*20*	*7*	*9*	*21*		*10*		
[7;50[	**0.30**	**0.24**	**0.17**						
n	*10*	*17*	*24*						

n: number of observed segments.

(Fig. 9). A greater or smaller part of the collector network was not eroded in a given year and some parts were never eroded during the study period.

Each segment of the runoff collector network was associated with the portion of rill lying within the precision interval of the segment location. We could therefore quantify (i) the percentage of rill volumes located on the collector network, and (ii) the eroded part of the network.

Table 7 confirms that most of the rill volumes lay on the pre-defined collector network. Rills lying outside the network had very small cross-sectional areas and generally belonged to parallel patterns developed on hillslopes and associated with linear agricultural features, such as wheel tracks or drilling lines. These features were not included in the design of the collector network and in the following analysis, as previously mentioned (Section 2.2.5). Conversely, most network segments were not associated with rills, but the proportion of non-eroded segments varied widely between catchments and between years.

We attempted to correlate the occurrence of erosion symptoms (only ephemeral gully and dendritic rill patterns) with the characteristics of corresponding segments. Disregarding the year and the catchment, the total population of segments identified in the first catchment sample was divided into 37 subgroups according to their runoff-contributing area (**RCA**) and slope gradient (**SL**) (Table 8). The proportion of segments without erosion (**PWE**) in each subgroup was calculated. It was not possible to split the subgroups by taking into account the grade of soil susceptibility to rill erosion (**SSE**) because there were too few segments in most subgroups.

Table 8 shows that **RCA** and **SL** strongly influence the proportion of non-eroded segments. This proportion was close to 1 when **RCA** was zero, regardless of the slope. Conversely, very low proportions of intact segments (0.10 to 0.30) were found when the

RCA was greater than 2 ha and **SL** was above 5%. **SL** had a greater influence when **RCA** was higher. Very low **SL** values did not counteract the influence of high values of **RCA**: values of **PWE** below 0.50 were found with **SL** lower than 2% when **RCA** was above 2 ha.

A description of the interactive influence of **RCA** and **SL** on the frequency of non-erosion cases was obtained by fitting the data in Table 8 to an equation of general form:

$$\mathbf{PWE} = (a\mathbf{RCA} + b)/((c\mathbf{SL} + d)\mathbf{RCA} + 1) \quad (1)$$

This form accounts for the dominant influence of **RCA**, the sharp change in **PWE** in response to **RCA** in the range of low **RCA** values, and the increasing influence of **SL** as **RCA** increased. Nonlinear regression was used to show that the minimum residual variance was associated with the following values:

$$a = 0.0606;\ b = 0.9205;\ c = 0.0918;\ d = 0.2752$$

with **RCA** in ha and **SL** in %. The residual standard deviation of **PWE** was 0.0909, while the initial standard deviation of **PWE** was 0.8272. The distribution of residual deviations to Eq. 1 (not shown) was independent of **SL**, but not of **RCA**: the frequency of non-erosion was slightly over-estimated by Eq. 1 when **RCA** was 2 to 7 ha, but slightly underestimated when **RCA** was over 7 ha. This might indicate that Eq. 1 is not perfectly appropriate for describing the drop in **PWE** when **RCA** increases. Unfortunately, the number of segments with **RCA** above 2 ha was too small (Table 8) for the **RCA** classes to be subdivided and the equation fitted to more detailed data.

Influence of segment characteristics on the cross-sectional area of rills

The average cross-sectional area of the rill portion contained within the precision interval of the segment location was obtained by dividing the rill volume by its length. Only rills with ephemeral gully or dendritic patterns were taken into account. The relationship between the segment characteristics and the cross-sectional area of rills (**CSA**) was studied by selecting the incised segments of the first catchment sample (76 in 1989/1990 and 187 in 1990/1991). The simple correlation coefficients (R) between **CSA** and **RCA**, **CSA** and **SL** and **CSA** and **SSE** were first calculated (Table 9). Only correlations with **RCA** were significant for the two winter seasons studied. The

Table 9
Coefficients of simple linear correlation (R) between the rill cross-sectional area (**CSA**) and the runoff-contributing area (**RCA**), the slope gradient (**SL**), and the soil susceptibility to rill erosion (**SSE**), at the segment scale

	RCA	SL	SSE
1989/1990 (n: 76) [a]	0.52*** [b]	−0.19* [b]	0.14^{ns} [b]
1990/1991 (n: 187)	0.50** [b]	0.18**	0.13*
1989/1990 and 1990/1991 (n: 263)	0.52***	0.08^{ns}	0.14**

[a] n: number of eroded segments.
[b] ***: $P < 1\%$; **: $P < 5\%$; *: $P < 10\%$; ^{ns}: $P > 10\%$.

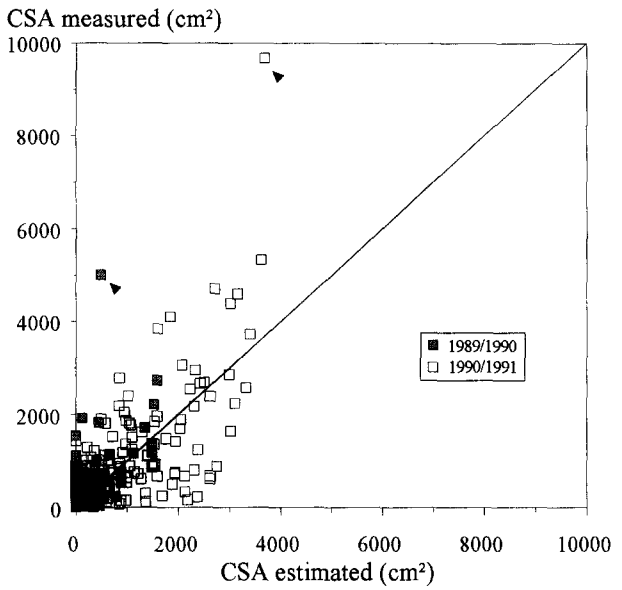

Fig. 10. Comparison of rill cross-sectional areas (**CSA**) measured in the field with the areas estimated from Eq. 2. Only eroded segments corresponding to winters 1989/1990 and 1990/1991 are taken into account (arrows indicate the same talweg portion for the two studied winters).

experimental data were then fitted to the following form of equation using a non-linear procedure:

$$\mathbf{CSA} = k\left(\left(\mathbf{RCA} \cdot 10^2\right)^l \cdot \mathbf{SL}^m \cdot \mathbf{SSE}^n\right) \quad (2)$$

with **CSA** in cm^2, **RCA** in ha, **SL** in % and **SSE** being a dimensionless number. This form of equation was chosen because the influence of **SL** and **SSE** was assumed to interact with the influence of **RCA**, and because zero values of one of these parameters were assumed to induce no erosion.

The numerical values of parameters k, l, m, n associated with the minimum residual variance of **CSA** were 1.93, 0.65, 0.78, 1.04 respectively. The determination coefficient for this particular equation was $R^2 = 0.44$; the standard deviation was 808.3 cm^2. These results were obtained without distinguishing between the two winter seasons ($n = 263$). The deviations between predicted and observed values of **CSA** appeared to be distributed in the same way for the two years (Fig. 10). The Kolmogorov–Smirnov test showed no significant difference ($P > 0.05$) between these two distributions of residuals. Moreover, the most important residuals for the two years (labelled points on Fig. 10) corresponded to the same segment, located in the central part of a talweg. This part of the talweg was always deeply eroded and filled up once or twice each year. Although a maximum **SSE** grade of 5 was attributed to this segment, this score could have underestimated the actual susceptibility of this segment. Lastly, the 1989/1990 results appeared to differ from those of 1990/1991 only by the lower values of **RCA** and not because of different influences of **RCA**, **SL** and **SSE** on **CSA**.

4. Discussion

4.1. Significance and limitations of the observed relationships

Rill initiation and development are threshold phenomena controlled by the hydrodynamic characteristics of the flow and by the topsoil cohesion. According to most authors (Savat and De Ploey, 1982; Govers, 1985; Govers and Rauws, 1986; Rauws and Govers, 1988; Everaert, 1991), the most relevant parameter describing the detaching ability of the flow is the shear velocity $\mathbf{U}^*$, which is positively linked to the slope (**SL**) and to the hydraulic radius of the flow (**R**):

$$\mathbf{U}^* = (\mathbf{g} \cdot \mathbf{R} \cdot \mathbf{SL})^{1/2}$$

where **g** is gravity. Scouring occurs when $\mathbf{U}^*$ exceeds a critical value $\mathbf{U}^*_{cr}$, which is related to soil characteristics. The hydraulic radius **R** depends on the flow discharge, and on the way this flow is spatially distributed.

In complex topographic conditions leading to flow concentration, the hydraulic radius of the flow for a given rainfall and in a given channel depends on the runoff-contributing area (**RCA**) associated with it, and on the cross-sectional shape of this channel. The threshold condition $\mathbf{U}^* > \mathbf{U}^*_{cr}$ is then related to a critical combination of **RCA** and **SL** for a given channel. At a catchment scale, the time and space distributions of rill heads along the runoff collector network will be controlled by the time and space distributions of runoff-contributing areas, and by the time and space distributions of topsoil cohesion and slope gradients along the runoff collectors. Once a rill is initiated, additional processes such as mass movements on sidewalls and headcut erosion, become involved in rill development. The soil mechanical properties to be considered are not only those of the surface layer, but those of the whole eroded profile. Thus rill development is more complex than rill initiation, but flow discharge, slope gradient and soil susceptibility to rill erosion remain the variables controlling the increase in rill cross-sectional area for a given storm (Moore and Foster, 1990).

Eqs. 1 and 2 indicate that the probability of rill incision of a given collector segment and the cross-sectional area of an actual rill increase when the runoff-contributing area (**RCA**), the slope gradient (**SL**) and the soil susceptibility to rill erosion (**SSE**) increase. These trends are in agreement with the physical influence of each of these factors, and the wide variations in each of them. This variability is particularly important for **RCA** and **SSE** in cultivated catchments, because they depend strongly on farm operations, which differ from field to field (Monnier et al., 1986; Boiffin et al., 1988b; Papy and Boiffin, 1988).

Eq. 1 describes rill initiation as a stochastic event taking into account the influence of **RCA** and **SL** by the probability of incision. This procedure is used because no information is available about other factors liable to influence rill initiation, e.g. those acting on flow channel shape. The influence of these unknown factors is considered to be a random black-box process.

Eq. 2 accounts for rill development in eroded channels. Less than a half of the total variance of the rill cross-sectional area is explained by Eq. 2. We must therefore examine the possible influence of factors not involved in Eq. 2. Theories of rill development imply that rainfall intensities is responsible for some part of the variability

of rill geometry. Rainfall intensities were certainly very different between catchments for the same season, and between years for the same catchment. Since they are not taken into account in Eq. 2, this could be a major source of residual variance. However, the residuals given by Eq. 2 do not depend on the year, although the rainfall characteristics of the two winters studied were very different. This indicates that a large part of the influence of rainfall is adequately expressed by the independent variables in the regression equation. Rainfall acts on soil erosion not only by generating runoff, but also by making the soil surface suitable for runoff generation by gradually breaking down soil surface structure, which results in an increase in **RCA**. **RCA** thus accounts for a large part of the cumulative influence of rainfall. However, the maximum width and depth of rills is mostly determined by the most important rain events (Moore and Foster, 1990). The variability of rainfall intensities during erosive storms is ignored by Eq. 2, and remains involved in the residual variance.

Eqs. 1 and 2 also take into account the hydrodynamic properties of the soil surface via the variable **RCA**, which expresses the area of fields having a strongly degraded surface structure. This procedure amounts to describing the susceptibility of land to runoff with only two options (yes/no), which is obviously very approximate. This potential source of residual errors is confirmed by considering the 55 eroded segments (i.e. 21% of the total number of eroded segments) having **RCA** values of zero. Twenty nine of these segments were connected to areas with moderately degraded surface structure, from which runoff was obviously generated. A more detailed analysis of factors determining rill presence and rill geometry should be based on a more flexible and graduated description of soil characteristics influencing runoff generation.

Other possible sources of error in the analysis of rill presence and geometry are:

- the qualitative and very rough estimation of **SSE**, which appears to be particularly poor in the case of repeatedly filled-in talwegs;
- errors in estimating the hydrological connection between runoff-contributing areas and the runoff collector network. This estimation is based mainly on topographical maps, while in some cases the actual connections were determined by microtopographic features;
- difficulties in describing the runoff-contributing areas of segments located downstream of a flow divergence. In such cases, the upslope **RCA** was arbitrarily subdivided in equal parts for each branch of the downslope collectors network, which could have been very different from the real flow distribution;
- not taking into account the influence of variations in runoff sediment concentration along the collector network. As the detachment capacity of the flow depends on its sediment load (Foster, 1990), the runoff erosive power could be lower in the downslope part of hillslopes.

From these considerations, it is clear that the approach used in this survey is much more convenient for analyzing changes in global erosion rates at a catchment scale, than for a detailed understanding of the local characteristics of rills.

4.2. Assessment of erosion rates on the catchment scale

Data on catchment erosion rates have generally been analysed taking a global approach, i.e. relating total or average erosion rates within a catchment to average

catchment characteristics (e.g. Auzet et al., 1993,1995). The effect of the catchment internal structure on erosion cannot be assessed when only total or average values are considered, and only part of the observed variation in erosion rate can be explained. The above analysis can be used to reconstruct the total volume of rills belonging to the "ephemeral gully" and "dendritic" patterns in a given catchment taking into account internal catchment structure, while allowing at the same time to estimate the accuracy of the predictions.

4.2.1. Estimation of rill volumes for the first catchment sample

The procedure consists of the following three steps.

1. Stochastic determination of rill presence or absence: the probability of a given collector segment, labelled subscript **i**, at a given moment, not being eroded ($\mathbf{PWE_i}$) is given by Eq. 1, knowing $\mathbf{SL_i}$ and $\mathbf{RCA_i}$ at this time. Knowing $\mathbf{PWE_i}$, the presence or absence of a rill is determined by randomly drawing a value from a series of numbers uniformly distributed between 0 and 1. The rill is present when $\alpha > \mathbf{PWE_i}$ and absent when $\alpha \leq \mathbf{PWE_i}$.

2. Determination of rill volume for eroded segments: the rill cross-sectional area ($\mathbf{CSA_i}$) is estimated from Eq. 2 and the associated value of residual variance. Knowing $\mathbf{RCA_i}$, $\mathbf{SL_i}$ and $\mathbf{SSE_i}$, an average estimate μ_i is given by Eq. 2. An additional term ϵ is drawn at random from a normal distribution with a zero mean value and a standard deviation of 808 cm^2. $\mathbf{CSA_i}$ equals $\mu_i + \epsilon$ when this algebraic sum is positive, or equals 0 when it is negative. The rill volume $\mathbf{V_i}$ of each eroded segment is estimated from the cross-sectional area, $\mathbf{CSA_i}$, and the segment length $\mathbf{L_i}$, assuming a simple parallelepipedic shape:

$$\mathbf{V_i} = \mathbf{CSA_i} \cdot \mathbf{L_i}$$

3. Determination of rill volume and erosion rate due to concentrated flow at the catchment scale: the total volume of rills belonging to the "ephemeral gully" and "dendritic" patterns in a given catchment **j** ($\mathbf{SCV_j}$) and the corresponding erosion rate $\mathbf{SCR_j}$ is given by:

$$\mathbf{SCV_j} = \Sigma_i \mathbf{V_{ij}}$$

$$\mathbf{SCR_j} = \mathbf{SCV_j}/\mathbf{CA_j}$$

where $\mathbf{CA_j}$ is the total area of catchment **j**.

This three-step procedure has been repeated 50 times for each catchment, providing an estimate of average $\mathbf{SCR_j}$ and a standard deviation. The standard deviations obtained in this way are about 0.6 $m^3 \cdot ha^{-1}$ for the least eroded catchments and 1.2 $m^3 \cdot ha^{-1}$ for the most eroded catchments ($\mathbf{SCR_j}$ below or above 3 $m^3 \cdot ha^{-1}$). As shown in Fig. 11, the average estimates of $\mathbf{SCR_j}$ were closely correlated with observed values. The regression equation is:

$$\mathbf{SCR_{jobs}} = -0.13 + 1.28\,\mathbf{SCR_{jest}} \quad (3)$$

with $R^2 = 0.90$ and a standard deviation of 0.72 m^3 ha^{-1}.

The intercept -0.13 is not significantly different from zero ($P > 0.05$), but the slope 1.28 is significantly different from 1 ($P < 0.01$), which means that the procedure

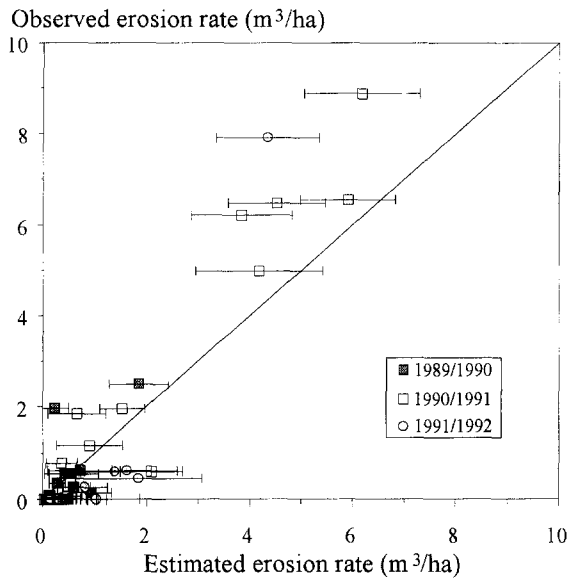

Fig. 11. Comparison of observed erosion rates (m^3/ha) at the catchment scale with erosion rates obtained by adding the rill volumes estimated for each segment.

systematically underestimates $\mathbf{SCR}_j$. This systematic bias originates from two main sources:

(i) a tendency to underestimate the very large cross-sectional area of talweg gullies. This trend appears in Fig. 10, where none of the estimated **CSA** values was above 4000 cm^2, although 7 observed values were higher. All these particular values corresponded to long talweg segments which exaggerated the underestimation of rill volumes. As mentioned above, the cross-sectional area of talweg gullies may be underestimated because the very high soil susceptibility to runoff detachment along the talweg was underestimated;

(ii) a tendency to underestimate the rill length of highly eroded segments. Since rill courses are not perfectly straight, segment lengths are generally shorter than the actual rill lengths. The opposite case (segment length greater than rill length) always corresponds to small rills starting within the segment, with low cross-sectional area. These cases have little influence on catchment rill volume, while rills with underestimated length effect the cumulated rill volume much more.

4.2.2. Application to the second catchment sample

The above procedure was applied to the second catchment sample to predict the erosion rates obtained in 1991/1992. Eqs. 1 and 2 were used without changing the coefficients obtained from the first set of data (1989/1990 and 1990/1991, first catchment sample). The results are plotted in Fig. 11 as additional points, labelled by circles.

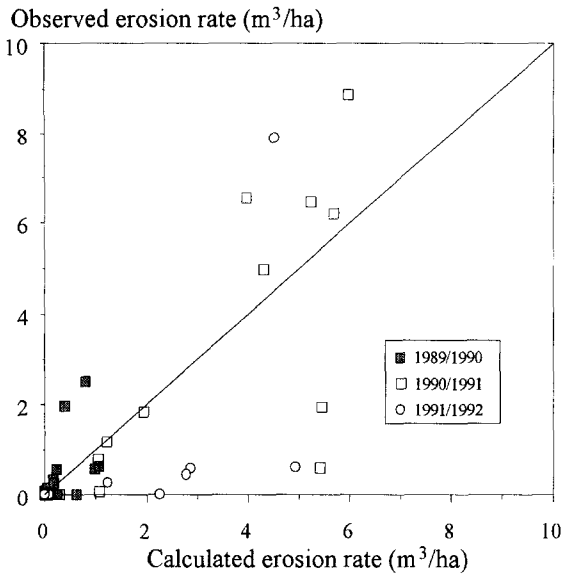

Fig. 12. Observed and calculated (Eq. 4) erosion rates (m^3/ha) at the catchment scale.

Unfortunately, the distribution of erosion rates for the second catchment sample was not really appropriate for validation, because most erosion rates were very low, with only one high value. However, the distribution of observed versus predicted values did not conflict with the distribution obtained with the first set of data.

4.2.3. Comparison to the global approach

In a previous study, Auzet et al. (1995) found a significant correlation between catchment erosion rates and an estimation of potential runoff-contributing area (**PR**), expressed as a percentage of the catchment area. No other topographical or soil feature appeared to have a significant influence on erosion rate when using this approach of global correlation between rill volumes and average catchment characteristics.

Using the same approach for the first catchment sample gave the following equation:

$$\mathbf{SCR}_j = 0.040\,\mathbf{PR}_j^{1.10} \quad (n = 40) \tag{4}$$

Erosion rates were clearly more poorly predicted by Eq. 4 ($R^2 = 0.68$) than by the whole procedure previously explained, as summarized by Eq. 3 ($R^2 = 0.90$). The results obtained using Eq. 4 to predict the erosion rates for the second catchment sample were also very different from the observed values. Comparison of Fig. 11 with Fig. 12 clearly demonstrates that the three-step procedure accounts for changes in erosion rate much better than does the correlative global approach, which ignored the internal hydrological structure of the catchment.

Because this structure is ignored, the global approach cannot take into account the limiting influence of potential rill lengths. Neither can it reveal the influence of local

conditions, such as slope or soil susceptibility to rill erosion, which are not properly taken into account at a catchment scale. As a result, this global approach cannot discriminate the potential for concentrated flow erosion between catchments having the same proportion of land with a degraded surface structure, but a very different collecting network.

5. Conclusion

The spatial units relevant to studies of concentrated flow erosion are zero order catchment, when referring to the permanent hydrological network. Their boundaries are generally defined by permanent topographic features. But within these permanent units, interactions between topographic and agricultural features determine a complex, temporary hydrological sub-structure.

The first component of this sub-structure is the runoff collector network. A part of this network is constituted by topographical linear features, such as talwegs or depression lines on hillslopes. The other part consists of agricultural linear features associated with field boundaries, such as headlands and dead furrows, which are prone to concentrate the overland flow coming from the fields and to direct it towards the main topographical collectors.

The second component of the internal hydrological structure of a catchment is the space distribution of runoff-contributing areas which varies with time. On a given field, the tendency for the land to generate runoff is controlled by changes in soil surface structure which result from interactions between farm operations, topsoil texture and rainfall. The spatial distribution of runoff-contributing areas at a given moment depends on the spatial distribution of the above mentioned factors and on the field pattern. The connections between the runoff-contributing areas and the collector network are determined by a complex system of local topographic conditions. Some of them cannot be identified without direct observation. Despite this complexity, adequate field observations combined with some simplifying hypothesis can be used to identify and characterize the runoff collectors, the runoff-contributing areas and their connections. It thus becomes possible to represent the catchment as a system of nested sub-units which is more appropriate for analyzing the variability of erosion features, than the whole catchment. Indeed, the control of rill volume by the collector length, the slope gradient and the soil cohesion can be taken into account for each sub-unit. The presence or absence of local hydraulic connections between runoff-contributing areas and runoff collectors can also be taken into consideration. The total catchment erosion rate is better explained and predicted as a sum of segment rill volumes, than by a global correlative approach.

The study described above was not strictly a modelling approach, since it was based on empirical relationships between rill geometry and selected land characteristics. However, the results obtained by this method show that any model developed to describe concentrated flow erosion in cultivated catchments should take into account their internal hydrological structure, which is determined not only by topography and soil properties, but also by agricultural land-use.

References

Auzet, A.V., Boiffin, J., Papy, F., Maucorps, J. and Ouvry, J.F., 1990. An approach to the assessment of erosion forms and erosion risk on agricultural land in the Northern Paris Basin, France. In: J. Boardman, I.D.L. Foster and J.A. Dearing (Editors), Soil Erosion on Agricultural Land. Wiley, Chichester, pp. 383–400.

Auzet, A.V., Boiffin, J., Papy, F., Ludwig, B. and Maucorps, J., 1993. Rill erosion as a function of the characteristics of cultivated catchments in the north of France. Catena, 20: 41–62.

Auzet, A.V., Boiffin, J. and Ludwig, B., 1995. Concentrated flow erosion in cultivated catchments: influence of soil surface state. Earth Surf. Process. Landforms, in press.

Baize, D., 1993. Soil Science Analysis. A Guide to Current Use. Wiley, Chichester, 250 pp.

Boardman, J., 1990. Soil erosion in the South Downs: a review. In: J. Boardman, I.D.L. Foster and J.A. Dearing (Editors), Soil Erosion on Agricultural Land. Wiley, Chichester, pp. 87–105.

Boiffin, J., 1986. Stages and time-dependency of soil crusting in situ. In: F. Callebaut, D. Gabriels and M. De Boodt (Editors), Assessment of Soil Surface Sealing and Crusting. Departement of Soil Physics, State University of Ghent, Ghent, pp. 91–98.

Boiffin, J., Papy, F. and Eimberck, M., 1988a. Influence des systèmes de culture sur les risques d'érosion par ruissellement concentré: I. Analyse des conditions de déclenchement de l'érosion. Agronomie, 8: 663–673.

Boiffin, J., Papy, F. and Monnier, G., 1988b. Some reflexions on the prospect of modelling the influence of cropping systems on soil erosion. In: R.P.C. Morgan and R.J. Rickson (Editors), Agriculture: Erosion assessment and modelling. CEE Report 10860, pp. 215–234.

Chen, Y., Tarchitzky, J., Brouwer, J., Morin, J. and Banin, A., 1980. Scanning electron microscope observations on soil crusts and their formations. Soil Science, 130: 49–55.

De Ploey, J., 1989. Erosional systems and perspectives for erosion control in European loess areas. In: U. Schwertmann, R.J. Rickson and K. Auerswald (Editors), Soil ersoion protection mesures in Europe. Soil Technology Series, 1. Catena Verlag, Cremlingen-Destedt, pp. 93–102.

Everaert, W., 1991. Empirical relations for the sediment transport capacity of interrill flow. Earth Surf. Process. Landforms, 16: 513–532.

Foster, G.R., 1986. Understanding ephemeral gully erosion. In: Soil Conservation, Assessing the National Inventory, Vol. 2. Academic Press, Washington, DC, pp. 90–125.

Foster, G.R., 1990. Process-based modelling of soil erosion by water on agricultural land. In: J. Boardman, I.D.L. Foster and J.A. Dearing (Editors), Soil erosion on agricultural land. Wiley, Chichester, pp. 429–445.

Govers, G., 1985. Selectivity and transport capacity of thin flows in relation to rill erosion. Catena, 12: 35–49.

Govers, G. and Rauws, G., 1986. Transporting capacity of overland flow on plane and irregular beds. Earth Surf. Process. Landforms, 11: 515–524.

Govers, G., Everaert, W., Poesen, J., Rauws, G., De Ploey, J. and Lautridou, J.P., 1990. A long flume study of the dynamic factors affecting the resistance of a loamy soil to concentrated flow erosion. Earth Surf. Process. Landforms, 15: 313–328.

Guerif, G., 1990. Conséquence de l'état structural sur les propriétés et les comportements physiques et mécaniques. In: J. Boiffin and A. Marin-Laflèche (Editors), La Structure du Sol et Son Evolution: Conséquences Agronomiques, Maîtrise par l'Agriculteur. Les Colloques de l'INRA 53. INRA, Paris, pp. 71–89.

Imeson, A.C. and Kwaad, J.P.M., 1990. The response of tilled soils to wetting by rainfall and the dynamic character of soil erodibility. In: J. Boardman, I.D.L. Foster and J.A. Dearing (Editors), Soil Erosion on Agricultural Land. Wiley, Chichester, pp. 3–14.

Jamagne, M., 1967. Bases et techniques d'une cartographie des sols. Ann. Agron., 18 (hors série), 142 pp.

Lyle, W.M. and Smerdon, E.T., 1965. Relation of compaction and other properties to resistance of soils. Trans. Am. Soc. Agric. Eng., 8: 419–422.

Monnier, G. and Boiffin, J., 1986. Effect of the agricultural use of soils on water erosion: the case of cropping systems in western Europe. In: C. Chisci and R.P.C. Morgan (Editors), Soil Erosion in the European Community. Balkema, Rotterdam, pp. 210–217.

Monnier, G., Boiffin, J. and Papy, F., 1986. Réflexions sur l'érosion hydrique en conditions climatiques et topographiques modérées: cas des systèmes de grande culture de l'Europe de l'Ouest. Cah. ORSTOM, Sér. Pédol., 22: 123–131.

Moore, I.D. and Foster, G.R., 1990. Hydraulics and overland flow. In: M.G. Anderson and T.P. Burt (Editors), Process Studies in Hillslope Hydrology. Wiley, Chichester, pp. 215–254.

Ouvry, J.-F., 1990. Effet des techniques culturales sur la susceptibilité des terrains à l'érosion par ruissellement concentré: Expérience du Pays de Caux (France). Cah. ORSTOM, Sér. Pédol., 25: 157–169.

Papy, F. and Boiffin, J., 1988. Influence des systèmes de culture sur les risques d'érosion par ruissellement concentré: II. Evaluation des possibilités de maîtrise du phénomène dans les exploitations agricoles. Agronomie, 8: 745–756.

Papy, F. and Boiffin, J., 1989. The use of farming systems for the control of runoff and erosion. In: U. Schwertmann, R.J. Rickson and K. Auerswald (Editors), Soil Erosion Protection Measures in Europe. Soil Technology Series, Vol. 1, pp. 29–38.

Papy, F. and Douyer, C., 1991. Influence des états de surface du territoire agricole sur le déclenchement des inondations catastrophiques. Agronomie, 11: 201–215.

Poesen, J., 1993. Gully typology and gully measures in the European loess belt. In: S. Wicherek (Editor), Farm Land Erosion in Temperate Plains Environment and Hills. Elsevier, Amsterdam, pp. 221–239.

Poesen, J. and Govers, G., 1990. Gully erosion in the loam belt of Belgium: typology and control measures. In: J. Boardman, I.D.L. Foster and J.A. Dearing (Editors), Soil Erosion on Agricultural Land. Wiley, Chichester, pp. 513–530.

Rauws, G. and Govers, G., 1988. Hydraulic and soil mechanical aspects of rill generation on agricultural soils. J. Soil Sci., 39: 111–124.

Savat, J. and De Ploey, J., 1982. Sheetwash and rill development by surface flow. In: R. Bryan and A. Yair (Editors), Badland, Geomorphology and Piping. Geo Books, Norwich, pp. 113–126.

Thorne, C.R. and Zevenbergen, L.W., 1990. Prediction of ephemeral gully erosion on cropland in the South-eastern United States. In: J. Boardman, I.D.L. Foster and J.A. Dearing (Editors), Soil Erosion on Agricultural Land. Wiley, Chichester, pp. 447–460.